Perspective

Harvesting triplet excitons for near-infrared electroluminescence via thermally activated delayed fluorescence channel

You-Jun Yu,[1] Xue-Qi Wang,[1] Jing-Feng Liu,[1] Zuo-Quan Jiang,[1] and Liang-Sheng Liao[1,2,*]

SUMMARY

Near-infrared (NIR) emission is useful for numerous practical applications, such as communication, biomedical sensors, night vision, etc., which encourages researchers to develop materials and devices for the realization of efficient NIR organic light-emitting devices. Recently, the emerging organic thermally activated delayed fluorescence (TADF) emitters have attracted wide attention because of the full utilization of electron-generated excitons, which is crucial for achieving high device efficiency. Up to now, the TADF emitters have shown their potential in the deep red/NIR region. Considering the color purity and efficiency, however, the development of NIR TADF emitters still lags behind RGB TADF emitters, indicating that there is still much room to improve their performance. In this regard, this perspective mainly summarizes the past progress of molecular design on constructing TADF NIR emitters. We hope this perspective could provide a new vista in developing NIR materials and enlighten breakthroughs in both fundamental research and applications.

INTRODUCTION

Achieving near-infrared (NIR) emission is a fundamental and powerful means for numerous applications in the electronic field in modern life, such as night vision, biometric identification, sensor, optical communication, etc (Qian and Wang, 2010; Zampetti et al., 2019; Kim et al., 2018b). Such widespread and essential applications encourage the researchers to develop materials and physical mechanisms for the realization of NIR electroluminescence (EL) via organic light-emitting diodes (OLEDs) (Chen et al., 2020b; Zhang et al., 2018; Tao et al., 2014), which is considered as one of the promising candidates for the next-generation luminescence technology (Wang et al., 2020; Zhang et al., 2020a; Yang et al., 2017).

The first practical OLED with sandwich architecture was firstly reported by C.W. Tang and S. A. VanSlyke (Tang and VanSlyke, 1987). Such a simple but constructive scheme has great potential used in display and lighting, which have shown extensive attention for both basic research and commercial utilizations. As for the development of OLEDs, one main issue is how to utilize all electrogenerated excitons for EL.

TRIPLETS HARVESTING FOR HIGH DEVICE EFFICIENCY

Phosphorescence

As shown in Figure 1, there are 25% singlet excitons and 75% triplet excitons generated in the emitting layer (EML) of an OLED device. The initial fluorescence emitters can only utilize 25% singlet excitons, which inspires researchers to utilize nonradiative triplet excitons to satisfy commercial parameters. Furthermore, the organic metal complex, with the incorporation of heavy metals (such as Pt, Ir, Os, etc.), could utilize the triplet excitons through phosphorescence radiative transition with the enhanced spin-orbital coupling, which have been exploited for commercial applications. In the NIR region, phosphorescent emitters have also exhibited excellent device performance via triplet exciton utilization. In 2016, Tuong Ly et al. proposed a series of square-planar Pt(II) complexes that featured metal-metal-to-ligand charge transfer transition. This unique intermolecular luminescence mode resulted in state-of-the-art device performance with a 24% external quantum efficiency (EQE) and a peak at 740 nm (Tuong Ly et al., 2016). Molecular modification could lead to redshift emission. In 2020, Wei et al. pointed out that such well-ordered packing produced

[1]Institute of Functional Nano & Soft Materials (FUNSOM), Jiangsu Key Laboratory for Carbon-Based Functional Materials & Devices, Soochow University, 199 Ren'ai Road, Suzhou, Jiangsu 215123, P. R. China

[2]Macao Institute of Materials Science and Engineering, Macau University of Science and Technology, Taipa, Macau SAR 999078, China
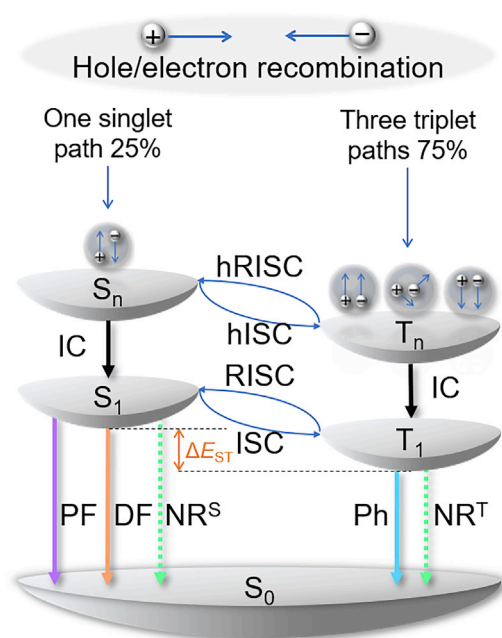
*Correspondence: lsliao@suda.edu.cn

https://doi.org/10.1016/j.isci.2021.102123

Figure 1. Jablonski diagram about triplet exciton utilization in pure organic system

PF, DF, Ph, NR^S, NR^T, IC, ISC, RISC, hISC, and hRISC represent prompt fluorescence, delayed fluorescence, phosphorescence, singlet nonradiative transition, triplet nonradiative transition, internal conversion, intersystem crossing, reverse intersystem crossing, intersystem crossing from the higher singlet states, and RISC from the higher triplet states, respectively.

weak electronic coupling, which contributed to efficient NIR emission. The Pt(II) complex named 4^tBu has realized an EQE of 2.14% with a peak at 930 nm (Wei et al., 2020).

Inspired by the unmatched device performance achieved by the organic complex system, pure organic compounds without heavy metal have also shown significant progress. An alternative strategy for triplet exciton utilization is to transfer the triplet excitons to the singlet state via the reverse intersystem crossing (RISC) process for fluorescence radiative transition. The rapid development of these materials has come up with prosperity in terms of facile synthesis and lower material cost. According to the position where the RISC process occurred, there are two kinds of classic mechanisms. One is called hybridize local and charge transfer (HLCT) (Li et al., 2012), and another is called thermally activated delayed fluorescence (TADF) (Uoyama et al., 2012).

Hybridize local and charge transfer

HLCT materials harvest triplets through the RISC process at a higher excited energy level. This kind of process is also known as the hot exciton channel. Typically, the utilization of triplet excitons from the hot exciton channel relies on the fine management of triplet energy level. Both a small energy splitting between the high singlet/triplet state and a large energy difference between the high triplet state/T_1 state are needed (Pan et al., 2014). Furthermore, the S_1 state should rationally hybridize both local and charge transfer components for both high radiative rate and high exciton utilization (Xu et al., 2019). In 2019, Jiang et al. reported an NIR HLCT emitter named DTPS-PT. The planner configuration of DTPS-PT, realized by small steric hindrance of thiophene, not only enhanced the π conjugation but also facilitated the hybridization of local excited and charge transfer component of the S_1 state. The optimal device based on DTPS-PT realized a high radiance of 2202 mW Sr^{-1} m^{-2} with a peak at 840 nm (Jiang et al., 2019). The fluorescence decay process of the HLCT emitter makes no difference from the conventional fluorescence emitter due to the fast RISC rate that occurred at high excited states. Considering the design principle, the previous works without relative analyses may also have HLCT properties.

Thermally activated delayed fluorescence

The exciton utilization of metal-free organic TADF emitters can also approach 100% exciton utilization through the RISC process from the T_1 state to the S_1 state (Chen et al., 2019). One key issue to boost this RISC process is minimizing the energy splitting between T_1 and S_1 (ΔE_{ST}). In that case, the spin-flip process of triplet excitons can easily be done. One general design strategy to minimize the ΔE_{ST} is separating

the frontier molecular orbitals (FMOs) by constructing a twisted donor-acceptor (D-A) configuration (Li et al., 2018; Cui et al., 2017). And the recent works indicate that the efficient RISC process also highly relies on the considerable spin-orbital coupling between the relatively excited states, which is dependent on the heteroatom in the molecular skeleton (Samanta et al., 2017; Guo et al., 2020). The twisted D-A structure has been demonstrated very effective in the visible region (Lin et al., 2016; Zeng et al., 2018; Chen et al., 2018; Zhang et al., 2019). The extraordinary device efficiency achieved in the visible region also encourages researchers to construct TADF emitters with efficient NIR emission.

ENERGY GAP LAW

When the bandgap redshifts to the NIR region, how to maintain high fluorescence efficiency should be thoroughly considered for all-type mechanisms. According to the energy gap law (Equation 1), the non-radiative transition rates increasing rapidly following the high probability of vibrational manifolds coupling between the ground states and the excited states (Englman and Jortner, 1970), which makes the design of NIR materials harder. The simplified form for non-radiative transition rate could be described as follows:

$$k_{nr} \propto exp\left(- \frac{\gamma \Delta E}{\hbar \omega_M} \right)$$

(Equation 1)

where ΔE is the energy gap between the two potential minima of the states, γ is a term that can be expressed in terms of molecular parameters, and ω_M is the maximum and dominant vibrational frequency.

RESEARCH PROGRESS OF NIR TADF EMITTERS

Generally, the highly twisted structure required for small ΔE_{ST} is not beneficial for redshifting the emission. Thus, to construct efficient NIR TADF emitters, the exploration of acceptor moieties with strong electron-withdrawing ability should be handled at first. The rigid and planar fused heterocycles for the acceptor are normally used. It is not only the ΔE_{ST} but also the fluorescence efficiency that should be considered simultaneously. The twisted D-A structure utilized for RGB emitters led to the decreased oscillator strength, facilitating the vibrational coupling between excited and ground state, which is harmful to the radiative transition. With the decreasing bandgap in the NIR region, the trade-off between the small ΔE_{ST} and high fluorescence efficiency is extremely challenged due to the more serious non-radiative energy loss. This inherent contradiction leads to the dilemma of the TADF mechanism in the NIR region.

Single molecular modifications for NIR TADF

One practical strategy widely employed is introducing a phenylene linker (Ph) to construct D-Ph-A type emitter for modifying the intramolecular charge transfer (ICT) interaction (Zhang et al., 2014). Compared with the D-A type emitter, the embedding phenylene linker could produce red-shifted emission by a larger dipole moment (Wang et al., 2017). In addition, the phenylene linker could also make the FMOs have a rational overlap, which usually provided a faster radiative rate without larger the ΔE_{ST} than the D-A type emitter. In 2015, Wang et al. reported a TADF emitter named TPA-DCPP with a narrow bandgap, which realized an EQE of 2.1% with a peak at 710 nm in a non-doped device (Wang et al., 2015). Detailed, the introduction of the phenylene linker not only realized a twisted structure causing a small ΔE_{ST} of 0.13 eV to support efficient RISC process but also resulted in the emitter to exhibit aggregate induced emission (AIE) properties, which avoided the concentration quenching.

In 2017, our group proposed a V-shaped emitter APDC-DTPA (Figure 2), which utilized acenaphtho[1,2-b]pyrazine-8,9-dicarbonitrile (APDC) as the acceptor for further red-shifted emission (Yuan et al., 2017). The stronger electron-withdrawing ability, compared with dibenzo[f,h]quinoxaline-2,3-dicarbonitrile (DCPP) (Wang et al., 2015), is resulted from the trend to form a more stable (4N + 2) cyclopentadienyl anion according to the Hückel rule. Moreover, the introduction of donor parts at 3 and 4 positions caused a suitable localization of the FMOs following a small ΔE_{ST} of 0.14 eV. The doped device created a recorded EQE of 10.19% with a peak at 693 nm. To improve device efficiency, we also explored the solvent effect of different hosts in aggregate states. The doped device with embedded APDC-DTPA in $Zn(BTZ)_2$ can harvest further redshift emission with high device efficiency (peak at 728 nm and an EQE of 5.1%).[32] The unique molecular structure and excellent performance of APDC-DTPA have encouraged researchers to explore acenaphtho[1,2-b]pyrazine derivatives for photo electricity functional materials (Gong et al., 2020a, 2020b; Li et al., 2020b). In 2019, Congrave et al. proposed a D-A dyad emitter, CAT-1, which could be considered as replacing one triphenylamine unit with a cyan group in APDC-DTPA (Yuan et al., 2017; Congrave et al.,
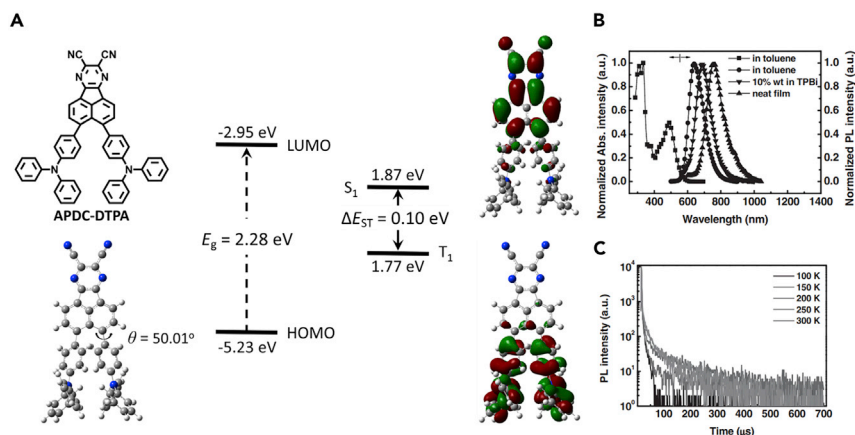
Figure 2. Structure and photophysical properties of ADPC-DTPA

(A) Chemical structure, optimized geometry, highest occupied molecular orbital (HOMO) and lowest unoccupied molecular orbital (LUMO) distributions, and calculated HOMO, LUMO, singlet (S_1), and triplet (T_1) energy levels of APDC-DTPA.

(B) UV-vis absorption and PL spectra of APDC-DTPA in toluene, neat and doped films, respectively.

(C) Temperature-dependent transient PL decays from 100 to 300 K for TPBi: APDC-DTPA doped film at 10 wt% concentration.

Figures reproduced from Yuan et al. (Yuan et al., 2017). Copyright 2017, WILEY-VCH.

2019). The ICT could greatly be strengthened and contributed to the impressive EL peak of 904 nm. The introduction of cyan groups on acceptor is a practical strategy for NIR TADF emitters. In 2020, Kumsampao et al. proposed a D-A-D type emitter based on a 5,6-dicyano[2,1,3]benzothiadiazole (Kumsampao et al., 2020). A deep red/NIR emission with a peak at 712 nm could attribute to the strong electron-withdrawing ability of the acceptor 5,6-dicyano[2,1,3]benzothiadiazole. The rational distribution of FMO would produce a high EQE of 6.56%.

Different from the above mentioned twisted molecular structure strategies for separating the FMOs, in 2018, Kim et al. reported a boron difluoride curcuminoid derivative, which exhibited nearly 10% EQE with a peak at 721 nm (Kim et al., 2018a). They proposed that the RISC process could occur via a non-adiabatic coupling effect for the utilization of triplet exciton. Moreover, the effective wavefunction overlap in the excited states contributed to high fluorescence emission. Soon later, Ye et al. reported the dimeric derivative, which exhibited an EQE of 5.1% with a red-shifted peak at 758 nm (Ye et al., 2018). Besides, both derivatives mentioned in the two works exhibited low threshold amplified spontaneous emission in the NIR region. In 2018, Higginbotham et al. reported a TADF molecule, named TPA-cNDI, based on naphthalene diimide core (Higginbotham et al., 2018). They found that the planar configuration caused a local triplet state, which contributes to the RISC process. The device based on TPA-cNDI realized a deep red/NIR emission with an EQE of 2.7%.

Utilization of intermolecular interaction

Beyond the single molecular design, the universal intermolecular interaction in the aggregation states would also be utilized to construct the TADF channel. In 2017, Li et al. reported a TADF emitter named TPA-QCN (Li et al., 2017). They pointed out that the red-shifted emission and weak quenching could be achieved simultaneously by the asymmetric molecule structure and edge-to-edge packing. The non-doped device achieved an EQE of 3.9% with a peak at 728 nm. In 2019, Xue et al. reported two pyridine derivatives named TPAAP and TPAAQ (Figure 3), which could realize TADF properties via J-type aggregates (Xue et al., 2019). Specifically, they found that the monomer did not show delayed fluorescence, proved by the decay curves in dilute toluene. The ΔE_{ST} values could be decreased for meeting the requirement of the RISC process through increasing doping ratio in the aggregate state, which caused gradually red-shifted fluorescence spectra. Furthermore, TPAAP exhibited an EQE of 14.1% (700 nm) and 5.1% (765 nm) in a doped and non-doped device, respectively. In the next year, Liang et al. reported a pyrazino[2,3-b]pyrazine derivative named TPAAZ, which maintained a related J-type packing mode (Liang et al., 2020). Benefitted from the stronger ICT interaction in the monomer, the emission peak of the non-doped device based on the TADF emitter TPAAZ firstly realized NIR-II emission with a peak at 1010 nm.
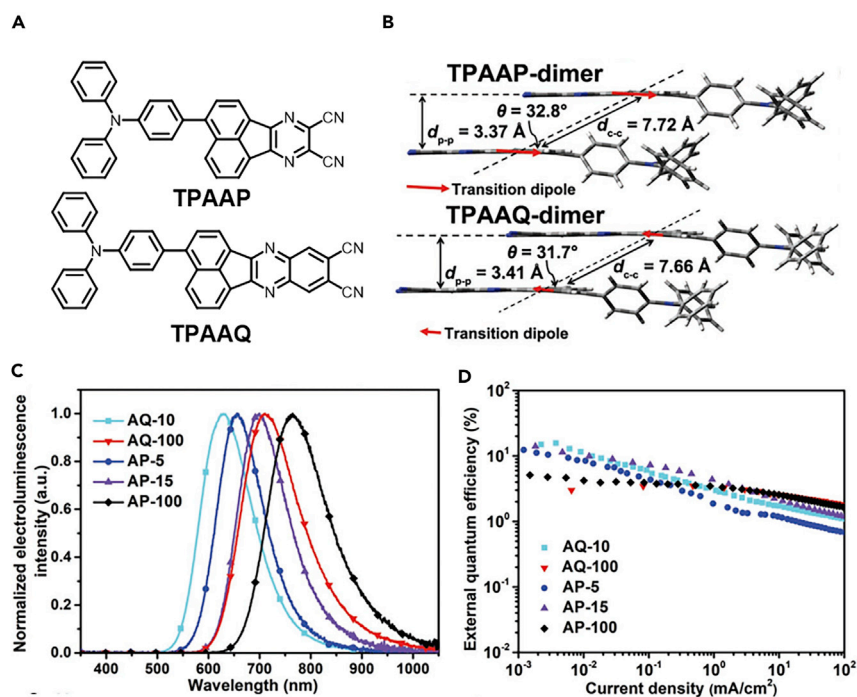
Figure 3. Structure and device performance of TPAAP and TPAAQ

(A) Chemical structures of TPAAP and TPAAQ.

(B) Packing patterns of aggregated dimers of TPAAP and TPAAQ with transition dipoles of S_1 represented by red arrows. The transition dipoles of S_1 were obtained by the time-dependent density functional theory (TD-DFT) approach at the level of TD/B3LYP/6-31G.

(C) EL spectra of the devices based on AQ-10 (10 wt% TPAAQ:TPBi as EML) and AP-5 (5 wt% TPAAP:TPBi as EML) at 5.4 V and that of the devices based on AP-15 (15 wt% TPAAP:TPBi as EML), AQ-100 (neat TPAAQ film as EML), and AP-100 (neat TPAAQ film as EML) at 3.2 V, respectively.

(D) EQE-current density (J) curves.

Figures reproduced from Xue et al. (Xue et al., 2019). Copyright 2019, WILEY-VCH.

Another well-known intermolecular strategy is the exciplex system, which is typically composed of hole and electron transporting materials (Sarma and Wong, 2018; Zhang et al., 2021a). With the blending of these components, an intermolecular charge transfer state would form with distinct red-shifted emission, which is an ideal approach for the utilization of the RISC process with an inherent small ΔE_{ST}. Exciplex systems would simplify the synthesis for the delicate molecular structures. In 2016, Data et al. proposed a dibenzo[a,j]phenazine derivative named POZ-DBPHZ with TADF characteristics (Data et al., 2016). Blending 10% POZ-DBPHZ in m-MTDATA could realize an efficient exciplex emission with a peak at 741 nm and an EQE of about 5%. In 2020, our group reported a series NIR exciplex system based on a fluorescence material, APDC-tPh, which possesses a low LUMO level (Hu et al., 2020). The exciplex-based devices exhibited turntable emission from 615 to 945 nm by changing various donors (m-MTDATA, Zn(BTZ)$_2$, TCTA, and CBP). With the utilization of a TADF emitter, TXO-TPA, as the donor, the exciplex-based device achieved an EQE of 1.27% with a peak at 704 nm.

Hyperfluorescence device

The main obstacles to obtaining the ideal NIR TADF emitters can be concluded in two aspects. One is the strong ICT required for NIR emission resulting in ultra-broad spectra. Another is low photoluminescence quantum yield (PLQY). An alternative strategy is separating the RISC process and radiative transition in a sensitizer and emitter, respectively, which would evade the inherent design confliction of TADF. In 2014, the conception of a TADF sensitizer was proposed by Adachi's group (Nakanotani et al., 2014). This strategy gives light to combining a TADF sensitizer with a fast RISC rate and guest emitters with required luminescence properties through Förster resonance energy transfer (FRET) for extraordinary device
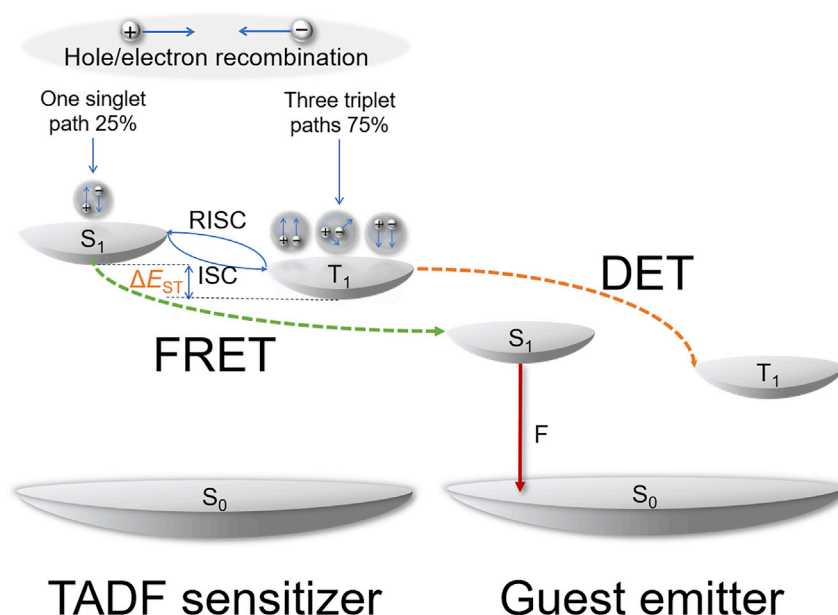
Figure 4. The energy transfer process for hyperfluorescence with TADF as a sensitizer
FRET and DET represent Förster resonance energy transfer and Dexter energy transfer, respectively.

performance (Figure 4). Typically, efficient spectra overlap between the PL spectra of the sensitizer and the absorption spectra of the emitter is needed for facilitating the FRET process. In 2017, Nagata et al. reported that TADF material can serve as a host matrix for both balanced carrier transporting and triplet harvesting (Nagata et al., 2017). With the utilization of the TADF host (PXZ-TRZ), CuPc- and PtPc-based devices exhibited improved device efficiency compared with Alq$_3$ as host. In the same year, Yamanaka et al. demonstrated that the sensitized NIR devices, in which TADF emitter named TPA-DCPP is used as a sensitizer and fluorescence emitter TPA-ThQ serves as an emitter, not only exhibited improved device efficiency but also showed good device stability. Moreover, the excellent device performance encouraged them to use the device as a lighting source for biosensing (Yamanaka et al., 2017). In 2017, Xue et al. reported TADF-sensitized NIR devices, in which DMAC-PN serves as the sensitized host and TPANSeD was chosen as the fluorescence emitter (Xue et al., 2017). The optimized sensitized device exhibited an EQE as high as 2.65% with a peak at 730 nm. In 2019, Brodeur et al. reported a TADF-sensitized NIR device, which exhibited a relative pure NIR emission with an NIR cut-on wavelength of 749 nm and more than 90% spectra fall into the region above 750 nm (Brodeur et al., 2019). In 2020, Shahalizad et al. reported a hyperfluorescent device (Figure 5), in which the NIR TADF emitter named TPAM-BF2 serves as a sensitizer for the pyrrolopyrrole cyanine dyes corded as BPPC-Ph (Shahalizad et al., 2020). The effective FRET process greatly improved the NIR narrowband emission origin from the BPPC-Ph and resulting in a 3.8% EQE with a peak at 840 nm and a full width at half maximum (FWHM) below 40 nm. The reported sensitized devices indicate that the hyperfluorescence device could provide a rational exciton utilization, which results in improved device efficiency.

PERSPECTIVE ON NIR TADF EMITTERS

The pure organic emitters based on the benzo(1,2-c:4, 5-c′)bis((1,2,5)thiadiazole derivatives have exhibited a stable EQE of 0.28% with a peak at 1080 nm (Qian et al., 2009). The high performance realized in the fluorophore indicates a large potential for the pure organic system. Until now, the organic NIR emitters with TADF characteristics have made revolutionary progress, showing their advantages for harvesting all excitons. The EQE of emerging NIR TADF emitters has surpassed the limitation of the initial fluorescence emitter (~5%). And the EL spectra have covered the range to NIR-II (above 1000 nm). Besides, the emerging TADF-sensitized device also exhibits the potential for higher device efficiency. These relative NIR device performances are summarized in Tables 1 and 2. A schematic diagram relating the material parameters, device performances, and material design methods is shown in Figure 6. Despite the significant improvements, there are still spaces that should be filled.
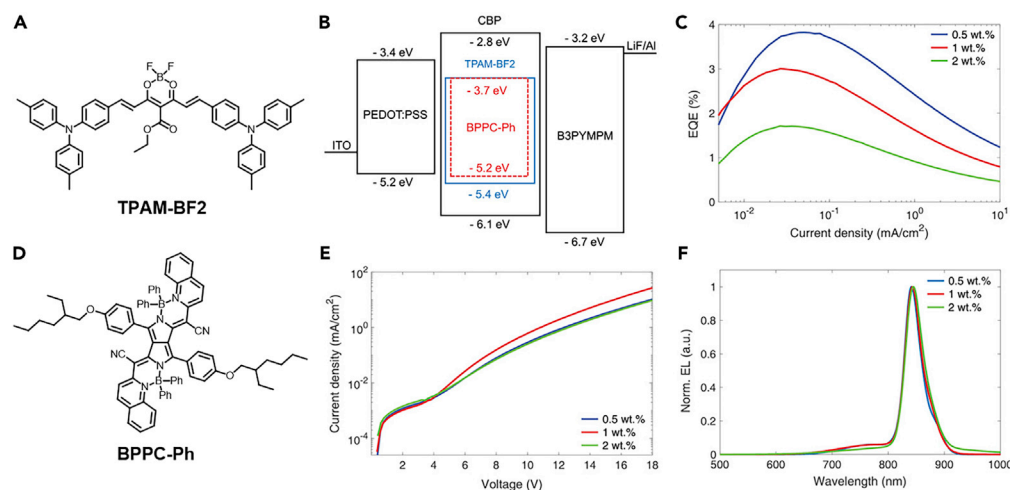
Figure 5. Materials and device performance of sensitized NIR OLEDs
(A) Chemical structure of TPAM-BF2.
(B) Energy level alignments of the materials used in the NIR OLEDs.
(C) EQE-*J* curves.
(D) Chemical structure of BPPC-Ph.
(E) *J*-*V* curves.
(F) EL spectra of the devices with CBP:TPAM-BF2 (20 wt%):BPPC-Ph (0.5, 1, 2 wt%) EML compositions and 80-nm-thick ETL.
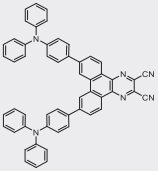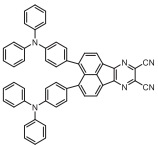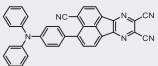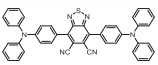Figures reproduced from Shahalizad et al. (Shahalizad et al., 2020). Copyright 2020, WILEY-VCH.
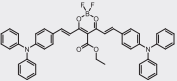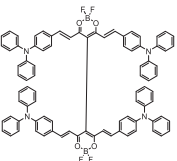
Realizing NIR EL with high spectroscopic purity

Up to now, most reported so-called "NIR" TADF emitters still contain visible tailing, and the emission bands are mainly located at NIR-I (700–1000 nm), which makes it hard to meet the spectrum requirement for practical applications (Yu et al., 2020). Such a spectrum needs an optical filter for modification, which usually decreases the device efficiency to a certain degree. On the one hand, most reported NIR emitters achieved the highest device efficiency in a doped device. Furthermore, increasing doping concentration could effectively redshift the emission; however, the device efficiency gets lose sharply. Such a phenomenon indicates that the aggregation-caused quenching is severe. A dilemma seems occurring for the pursuit of both a long emission peak and high efficiency. An AIE or aggregation-induced emission enhancement properties would be introduced for lessening fluorescence quenching at a high doping ratio (Zhao et al., 2020; Du et al., 2012). On the other hand, the FWHM of reported organic NIR TADF emitters still largely originates from the inherent strong ICT and twisted molecular structures. The emerging multiresonant TADF (MR-TADF) (Madayanad Suresh et al., 2020) and classic organic dyes, such as aza-BODIPY (Shimizu, 2019), owning both small Stokes shift and small FWHM would be suitable for exploring narrow NIR emission due to the rigid molecular configuration. An optional physics approach is utilizing microcavity efforts to narrow the emission band (Chen et al., 2010).

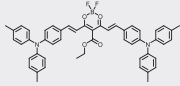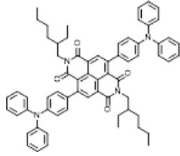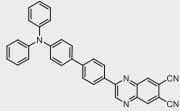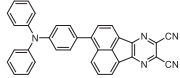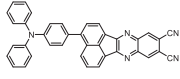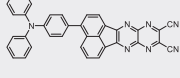### Constructing effective TADF channels for triplet utilization

An inefficient RISC process does make it hard to achieve high PLQY while the excessive intersystem crossing (ISC) process deactivates the singlet excitons. The rational alignment of twisted structure could produce effectively redshift EL without the loss of fluorescence efficiencies; however, indeed, indicating this strategy should be further revised to fit the narrow bandgap. The ideal NIR TADF should own high fluorescence efficiency and fast RISC process for both triplet exciton spin-flip and delayed fluorescence emission. With a deep understanding of the RISC process, it is not only a small ΔE_{ST} value but also a rational spin-orbital coupling that contributes to the effective triplet spin flip. The introduction of heteroatom could lead to high spin-orbital coupling between the two states. Moreover, it is the local excitation component in the triplet state (LE[3]) that mainly contributes to the charge-transfer demented singlet state (CT[1]) for NIR TADF emitters with twisted D-A structure (Chen et al., 2020a). Besides, the above mentioned TADF-sensitized process can also simplify the design conflicts.

Table 1. Summary of photophysical parameters and device performances of TADF emitters with EL peak above 700 nm.

Name	Structure	Host	Doping ratio[a]	PLQY[b] (%)	τ_p/τ_d[c] (ns/μs)	EQE$_{max}$[d] (%)	λ_{EL}[e] (nm)	L/J$_e$/L$_e$[f] (cd m^{-2}/ mW m^{-2}/mW Sr^{-1} m^{-2})	Ref.
TPA-DCPP		Non-doped	100	14	20.8/0.76	2.1	710	591/−/−	Wang et al. (2015)
APDC-DTPA		TPBi	10	17	−/−	10.19	693	−/−/-	Yuan et al. (2017)
		TPBi	20	63	−/−	9.70	696	−/−/-	
		Non-doped	100	17	−/−	2.19	777	−/−/-	
		Zn(BTZ)$_2$	10	59	−/−	7.8	710	−/−/-	Hu et al. (2018)
		Zn(BTZ)$_2$	20	51	−/−	5.1	728	−/−/-	
CAT-1		Non-doped	100	0.18	−/−	0.019	904	−/−/1000	Congrave et al. (2019)
TPACNBz		CBP	30	52	7/1.52	6.57	712	−/−/10,020	Kumsampao et al. (2020)
Curcuminoid derivative 1		CBP	6	70	2.3/28	9.69	721	−/−/500000	Kim et al., 2018a
Curcuminoid derivative 2		CBP	2	45.2	−/−	5.10	758	−/−/640000	Ye et al. (2018)

Table 1. Continued

Name	Structure	Host	Doping ratio[a]	PLQY[b] (%)	τ_p/τ_d[c] (ns/μs)	EQE$_{max}$[d] (%)	λ_{EL}[e] (nm)	L/J$_e$/L$_e$[f] (cd m^{-2}/ mW m^{-2}/mW Sr^{-1} m^{-2})	Ref.
TPAM-BF2		CBP	6	41.9	–/–	6.5	737	–/–/-	Shahalizad et al. (2020)
TPA-cNDI		CBP	10	–	1.2/10	2.4	–	-/27,000/-	Higginbotham et al. (2018)
TPA-QCN		TPBi	30	47	19.7/201	9.4	700	1371/–/–	Li et al. (2017)
		Non-doped	100	21	14.3/0.8	3.9	728	205/–/–	
TPAAP		TPBi	15	69.5	16.1/258	14.1	700	–/–/20,944	Xue et al. (2019)
TPAAQ		Non-doped	100	16.3	22.7/8.12	3.5	711	–/–/30,452	
TPAAZ		CBP	1	10.7	10.93/167.9	1.35	722	–/–/-	Liang et al. (2020)
		Non-doped	100	–	–/–	–	1010	–/–/-	

Table 1. *Continued*

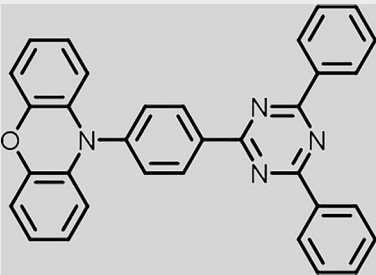| Name	Structure	Host	Doping ratio[a]	PLQY[b] (%)	τ_p/τ_d[c] (ns/µs)	EQE$_{max}$[d] (%)	λ_{EL}[e] (nm)	L/J$_e$/L$_e$[f] (cd m^{-2}/ mW m^{-2}/mW Sr^{-1} m^{-2})	Ref.
mMTDATA/ POZ-DBPHZ		Exciplex	90/10	–	–/–	5	741	35,000/–/–	Data et al. (2016)
TXOTPA/ APDC-tPh		Exciplex	50/50	9	-/0.318	1.27	704	–/–/13,000	Hu et al. (2020)
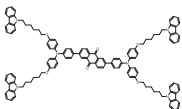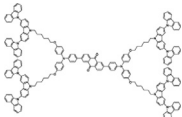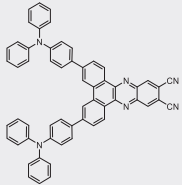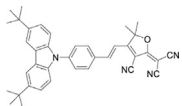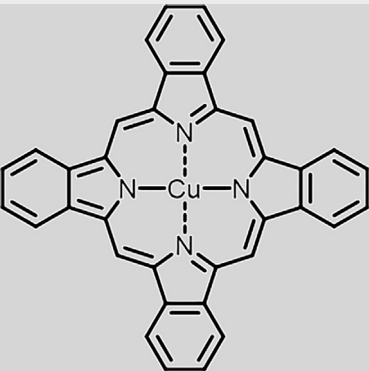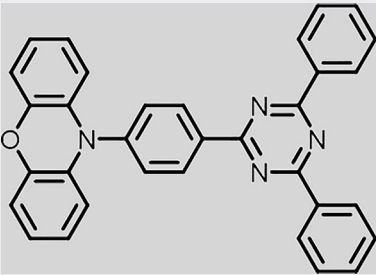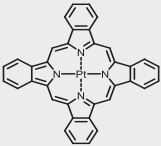
(Continued on next page)

Table 1. Continued

Name	Structure	Host	Doping ratio[a]	PLQY[b] (%)	τ_p/τ_d[c] (ns/μs)	EQE$_{max}$[d] (%)	λ_{EL}[e] (nm)	$L/J_e/L_e$[f] (cd m^{-2}/ mW m^{-2}/mW Sr^{-1} m^{-2})	Ref.
MPPA-Cz		Non-doped	100	6	-/0.56	0.064	728	24/—/—	Sun et al. (2017)
MPPA-3Cz		Non-doped	100	8	-/0.96	0.254	715	135/—/—	
DPA-Ph-DBPzDCN		mCPPy2PO	20	25	23.9/121.9	5.53	708	605/—/—	Wang et al. (2018)
		mCPPy2PO	30	14	25.3/101.1	3.94	720	383/—/—	
		mCPPy2PO	50	–	—/—	2.40	732	258/—/—	
tBCzTCF		Non-doped	100	26.6	—/—	0.3	715	—/—/-	Zhao et al. (2019)
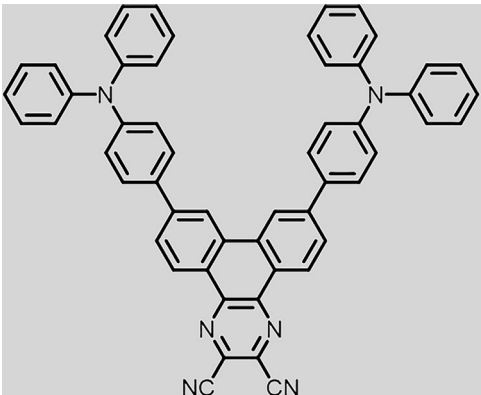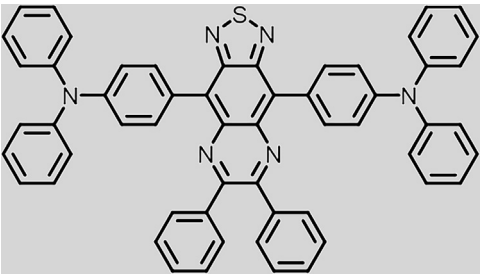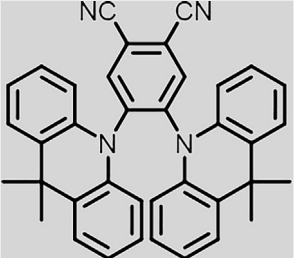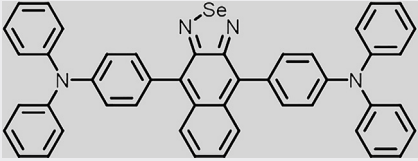
[a]Doing ratio in the corresponding host.
[b]Photoluminescence quantum yield of the corresponding film.
[c]Prompt fluorescence lifetime (τ_p)/delayed fluorescence lifetime (τ_d) of the corresponding film.
[d]Maximum external quantum efficiency of the OLED with the corresponding film as EML.
[e]Peak wavelength of electroluminescence spectra.
[f]Luminescence(L)/irradiance (J_e)/radiance (L_e) value of the OLED.

Table 2. Summary of photophysical parameters and hyperfluorescence device performances based on TADF sensitizer with EL peak above 700 nm.

Name[a]	Structure (TADF material)	Structure (guest emitter)	Doping ratio[b]	PLQY[c] (%)	EQE$_{max}$[d] (%)	λ_{EL}[e] (nm)	$\Phi_e/J_e/L_e$[f] (mW/ mW m^{-2}/mW Sr^{-1} m^{-2})	Ref.
PXZ-TRZ/ CuPc			99/1	–	0.03	1100	–/–/-	Nagata et al. (2017)
mCBP/ PXZ-TRZ/ CuPc			54/45/1	–	0.037	–	–/–/-	
PXZ-TRZ/ PtPc			99/1	0.3	0.1	970	–/–/-	

Table 2. Continued

Name[a]	Structure (TADF material)	Structure (guest emitter)	Doping ratio[b]	PLQY[c] (%)	EQE$_{max}$[d] (%)	λ_{EL}[e] (nm)	$\Phi_e/J_e/L_e$[f] (mW/ mW m^{-2}/mW Sr^{-1} m^{-2})	Ref.
CBP/TPA-DCPP/TPA-ThQ			79.5/20/0.5	–	3.3 (at 10 mA cm^{-2})	760	–/–/–	Yamanaka et al. (2017)
			49.5/50/0.5	–	3.3 (at 10 mA cm^{-2})	780	1/–/–	
DMAC-PN/TPANSeD			98/2	–	2.36	722	-/7830/-	Xue et al. (2017)
			96/4	–	2.65	730	-/10,569/-	
			94/6	–	2.11	731	-/24,624/-	
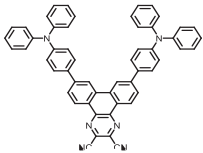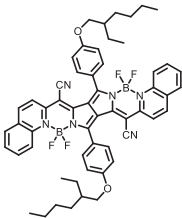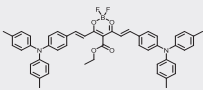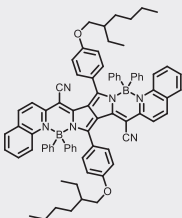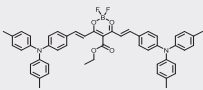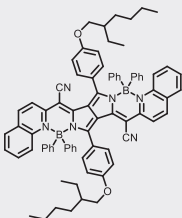
(Continued on next page)

Table 2. *Continued*

Name[a]	Structure (TADF material)	Structure (guest emitter)	Doping ratio[b]	PLQY[c] (%)	EQE$_{max}$[d] (%)	λ_{EL}[e] (nm)	$\Phi_e/J_e/L_e$[f] (mW/ mW m^{-2}/mW Sr^{-1} m^{-2})	Ref.
B3PYMPM/ TPA-DCPP/ DCPP			79.2/20/ 0.8	22	5.4	790	—/—/-	Brodeur et al. (2019)
TPBi/TPA-DCPP/DCPP			79.2/20/ 0.8	10	2.2	790	—/—/-	
CBP/TPAF-BF2/BPPC-Ph			79.5/20/ 0.5	15.8	3.5	840.7	—/—/-	Shahalizad et al. (2020)
			79/20/1	12.8	3	841	—/—/-	
			78/20/2	10.5	1.7	843.2	—/—/-	

[a]The material name used in binary (TADF host/emitter) or ternary (host/TADF sensitizer/emitter) film.

[b]Doping ratio for binary or ternary film.

[c]Photoluminescence quantum yield of the corresponding film.

[d]External quantum efficiency of the OLED with the corresponding film as the electroluminescence layer.

[e]Peak wavelength of electroluminescence spectra.

[f]Radiant flux (Φ_e)/Irradiance (J_e)/radiance (L_e) value of the OLED.
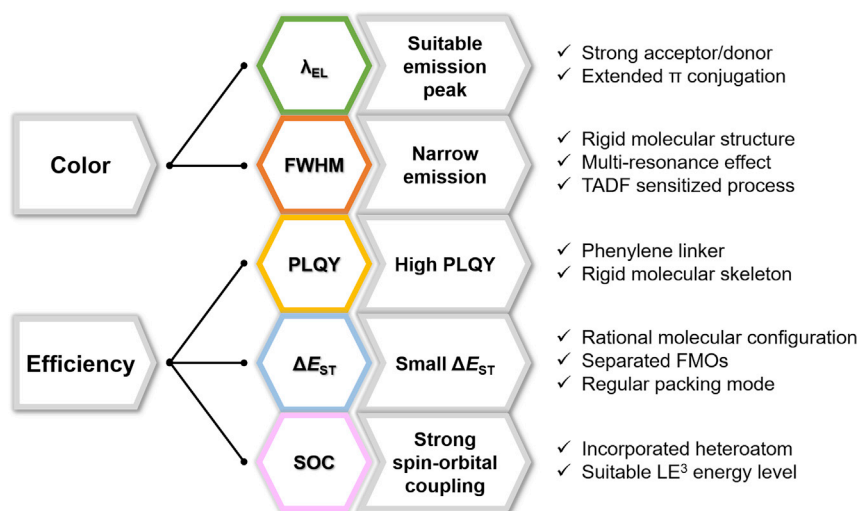
Figure 6. Schematic diagram relating the device performances, material parameters, and material design strategies

As for the molecular design, besides the classical ICT, the emerging through space charge transfer (TSCT) (Tang et al., 2020; Yang et al., 2020c; Peng et al., 2020; Wada et al., 2020; Tsujimoto et al., 2017; Li et al., 2020a), MR-TADF (Hatakeyama et al., 2016; Xu et al., 2020), and these hybridizations would be potential choices for the realization of efficient TADF channels in the NIR region in the future. As for the TSCT-based TADF emitters, electron donors and acceptors usually have a spatial face-to-face alignment through a rigid linker. The MR-TADF usually have a rigid polycyclic π-conjugated skeleton, in which, the acceptor units (usually the boron atoms or carbonyl groups) and donor units (nitrogen or oxygen atoms) are ortho-disposed for minimizing the ΔE_{ST}. When two MR-TADF segments are fused, the para-disposed acceptor/donor units could lead to red-shifted emission. For instance, a peak at 616 nm with an FWHM of 26 nm and an EQE_{max} of 22.0% was realized in an OLED device based on BBCz-R with para-disposed boron/nitrogen atoms in the central π-core (Yang et al., 2020a). And zhang et al. reported two MR-TADF emitters named R-BN and R-TBN, respectively, which exhibited deeper red emission of 664 and 686 nm with small FWHMs of 48 and 49 nm, respectively. Meanwhile, they have also realized high EQEs of 28.4 and 28.1%, respectively (Zhang et al., 2020b). As above mentioned, MR-TADF system materials have the potential to realize further red-shifted emission in the NIR region with the research and comprehension progressing. Besides, considering most reported NIR devices were realized in the non-doped device, the intermolecular interaction should also be considered, which could not only influence the RISC process but also affect the radiative process.

TADF mechanism for wide applications

Compared with quantum dots or perovskite materials, pure organic nature makes TADF emitters a better choice for applications in biomaterials (Kiyose et al., 2008). Furthermore, the high spatial and temporal resolution characteristics of NIR emission make NIR TADF emitters suitable for *in vivo* imaging (Qi et al., 2018). Moreover, the long-lived delayed fluorescence would also contribute to a better signal-noise ratio for time-resolved imaging (Ni et al., 2020). Considering the low fluorescence efficiency governed by the energy gap law, there is a large amount of energy in NIR TADF emitters converting to thermal energy, which could also be used for photothermal therapy (Alifu et al., 2018). On the other hand, the small ΔE_{ST} caused for delayed fluorescence could also generate singlet oxygen, which could be used for anticancer therapy (Yang et al., 2020b). Moreover, NIR TADF emitters could also be applied for chemical sensors due to large conjugation (He et al., 2019). Besides, the above mentioned NIR emitters (Kim et al., 2018a; Ye et al., 2018) have successfully been used for amplified spontaneous emission, which could be used for communication in the future.

OUTLOOK

Since the excellent device performance with visible emission was realized by the RISC process in TADF systems, the TADF channel for triplet utilization in the NIR region is going to emerge as the next research

topic. Hopefully, this perspective could help for the happening of design singularity for a TADF emitter, which leads to a practical device performance through efficient triplet utilization.

AUTHOR CONTRIBUTION

All the authors wrote and edited the manuscript.

DECLARATION OF INTERESTS

The authors declare no conflict of interest.

REFERENCES

Alifu, N., Zebibula, A., Qi, J., Zhang, H., Sun, C., Yu, X., Xue, D., Lam, J.W.Y., Li, G., Qian, J., and Tang, B.Z. (2018). Single-molecular near-infrared-II theranostic systems: ultrastable aggregation-induced emission nanoparticles for long-term tracing and efficient photothermal therapy. ACS Nano 12, 11282–11293.

Brodeur, J., Hu, L., Malinge, A., Eizner, E., Skene, W.G., and Kéna-Cohen, S. (2019). Highly efficient and spectrally narrow near-infrared fluorescent OLEDs using a TADF-sensitized cyanine dye. Adv. Opt. Mater. 7, 1901144.

Chen, J.X., Tao, W.W., Chen, W.C., Xiao, Y.F., Wang, K., Cao, C., Yu, J., Li, S., Geng, F.X., Adachi, C., et al. (2019). Red/near-Infrared thermally activated delayed fluorescence OLEDs with near 100 % internal quantum efficiency. Angew. Chem. Int. Ed. 58, 14660–14665.

Chen, J.X., Wang, K., Zheng, C.J., Zhang, M., Shi, Y.Z., Tao, S.L., Lin, H., Liu, W., Tao, W.W., Ou, X.M., and Zhang, X.H. (2018). Red organic light-emitting diode with external quantum efficiency beyond 20% based on a novel thermally activated delayed fluorescence emitter. Adv. Sci. 5, 1800436.

Chen, J.-X., Xiao, Y.-F., Wang, K., Sun, D., Fan, X.-C., Zhang, X., Zhang, M., Shi, Y.-Z., Yu, J., Geng, F.-X., et al. (2020a). Managing locally excited and charge-transfer triplet states to facilitate up-conversion in red TADF emitters that are available for both vacuum- and solution-processes. Angew. Chem. Int. Ed. 60, 2478–2484, https://doi.org/10.1002/anie.202012070.

Chen, S., Deng, L., Xie, J., Peng, L., Xie, L., Fan, Q., and Huang, W. (2010). Recent developments in top-emitting organic light-emitting diodes. Adv. Mater. 22, 5227–5239.

Chen, Z., Ho, C.-L., Wang, L., and Wong, W.-Y. (2020b). Single-molecular white-light emitters and their potential WOLED applications. Adv. Mater. 32, 1903269.

Congrave, D.G., Drummond, B.H., Conaghan, P.J., Francis, H., Jones, S.T.E., Grey, C.P., Greenham, N.C., Credgington, D., and Bronstein, H. (2019). A simple molecular design strategy for

delayed fluorescence toward 1000 nm. J. Am. Chem. Soc. 141, 18390–18394.

Cui, L.S., Nomura, H., Geng, Y., Kim, J.U., Nakanotani, H., and Adachi, C. (2017). Controlling singlet-triplet energy splitting for deep-blue thermally activated delayed fluorescence emitters. Angew. Chem. Int. Ed. 56, 1571–1575.

Data, P., Pander, P., Okazaki, M., Takeda, Y., Minakata, S., and Monkman, A.P. (2016). Dibenzo [a,j]phenazine-cored donor-acceptor-donor compounds as green-to-red/NIR thermally activated delayed fluorescence organic light emitters. Angew. Chem. Int. Ed. 55, 5739–5744.

Du, X.B., Qi, J., Zhang, Z.Q., Ma, D.G., and Wang, Z.Y. (2012). Efficient non-doped near infrared organic light-emitting devices based on fluorophores with aggregation-induced emission enhancement. Chem. Mater. 24, 2178–2185.

Englman, R., and Jortner, J. (1970). The energy gap law for radiationless transitions in large molecules. Mol. Phys. 18, 145–164.

Gong, X., Li, P., Huang, Y.H., Wang, C.Y., Lu, C.H., Lee, W.K., Zhong, C., Chen, Z., Ning, W., Wu, C.C., et al. (2020a). A red thermally activated delayed fluorescence emitter simultaneously having high photoluminescence quantum efficiency and preferentially horizontal emitting dipole orientation. Adv. Funct. Mater. 30, 1908839.

Gong, X., Lu, C.-H., Lee, W.-K., Li, P., Huang, Y.-H., Chen, Z., Zhan, L., Wu, C.-C., Gong, S., and Yang, C. (2020b). High-efficiency red thermally activated delayed fluorescence emitters based on benzothiophene-fused spiro-acridine donor. Chem. Eng. J. 405, 126663.

Guo, X., Yuan, P., Qiao, X., Yang, D., Dai, Y., Sun, Q., and Ma, D. (2020). Magneto-electroluminescence studies on the role of intermolecular spin-orbital coupling processes for the transition between singlet and triplet excitons in exciplex-based phosphorescent organic light-emitting diodes. Adv. Opt. Mater. 8, 2000991.

Hatakeyama, T., Shiren, K., Nakajima, K., Nomura, S., Nakatsuka, S., Kinoshita, K., Ni, J., Ono, Y., and Ikuta, T. (2016). Ultrapure blue thermally activated delayed fluorescence molecules: efficient HOMO-LUMO separation by the multiple resonance effect. Adv. Mater. 28, 2777–2781.

He, J.M., Yan, X.J., Liu, A., You, R., Liu, F.M., Li, S.Q., Wang, J., Wang, C.G., Sun, P., Yan, X., et al. (2019). A rapid-response room-temperature planar type gas sensor based on DPA-Ph-DBPzDCN for the sensitive detection of NH3. J. Mater. Chem. A. 7, 4744–4750.

Higginbotham, H.F., Pander, P., Rybakiewicz, R., Etherington, M.K., Maniam, S., Zagorska, M., and Data, P. (2018). Triphenylamine disubstituted naphthalene diimide: elucidation of excited states involved in TADF and application in near-infrared organic light emitting diodes. J. Mater. Chem. C 6, 8219–8225.

Hu, Y., Yu, Y.J., Yuan, Y., Jiang, Z.Q., and Liao, L.S. (2020). Exciplex-based organic light-emitting diodes with near-infrared emission. Adv. Opt. Mater. 8, 1901917.

Hu, Y., Yuan, Y., Shi, Y.-L., Li, D., Jiang, Z.-Q., and Liao, L.-S. (2018). Efficient near-infrared emission by adjusting the guest-host interactions in thermally activated delayed fluorescence organic light-emitting diodes. Adv. Funct. Mater. 28, 1802597.

Jiang, J.X., Xu, Z., Zhou, J.D., Hanif, M., Jiang, Q.L., Hu, D.H., Zhao, R.Y., Wang, C., Liu, L.L., Ma, D.G., et al. (2019). Enhanced pi conjugation and donor/acceptor interactions in D-A-D type emitter for highly efficient near-infrared organic light-emitting diodes with an emission peak at 840 nm. Chem. Mater. 31, 6499–6505.

Kim, D.H., D'Aleo, A., Chen, X.K., Sandanayaka, A.D.S., Yao, D.D., Zhao, L., Komino, T., Zaborova, E., Canard, G., Tsuchiya, Y., et al. (2018a). High-efficiency electroluminescence and amplified spontaneous emission from a thermally activated delayed fluorescent near-infrared emitter. Nat. Photon. 12, 98–104.

Kim, J.H., Yun, J.H., and Lee, J.Y. (2018b). Recent progress of highly efficient red and near-infrared

thermally activated delayed fluorescent emitters. Adv. Opt. Mater. 6, 1800255.

Kiyose, K., Kojima, H., and Nagano, T. (2008). Functional near-infrared fluorescent probes. Chem. Asian J. 3, 506–515.

Kumsampao, J., Chaiwai, C., Chasing, P., Chawanpunyawat, T., Namuangruk, S., Sudyoadsuk, T., and Promarak, V. (2020). A simple and strong electron deficient 5,6-dicyano[2,1,3]benzothiadiazole-cored donor-acceptor-donor compound as an efficient near infrared thermally activated delayed fluorescence. Chem. Asian J. 15, 3029.

Li, C., Duan, R., Liang, B., Han, G., Wang, S., Ye, K., Liu, Y., Yi, Y., and Wang, Y. (2017). Deep-red to near-infrared thermally activated delayed fluorescence in organic solid films and electroluminescent devices. Angew. Chem. Int. Ed. 56, 11525–11529.

Li, Q., Hu, J., Lv, J., Wang, X., Shao, S., Wang, L., Jing, X., and Wang, F. (2020a). Through-space charge transfer polynorbornenes with fixed and controllable spatial alignment of donor and acceptor for high-efficiency blue thermally activated delayed fluorescence. Angew. Chem. Int. Ed. 59, 20174.

Li, W.J., Liu, D.D., Shen, F.Z., Ma, D.G., Wang, Z.M., Feng, T., Xu, Y.X., Yang, B., and Ma, Y.G. (2012). A twisting donor-acceptor molecule with an intercrossed excited state for highly efficient, deep-blue electroluminescence. Adv. Funct. Mater. 22, 2797–2803.

Li, W., Li, Z., Si, C., Wong, M.Y., Jinnai, K., Gupta, A.K., Kabe, R., Adachi, C., Huang, W., Zysman-Colman, E., and Samuel, I.D.W. (2020b). Adv. Mater. 32, 2003911.

Li, Y., Liang, J.-J., Li, H.-C., Cui, L.-S., Fung, M.-K., Barlow, S., Marder, S.R., Adachi, C., Jiang, Z.-Q., and Liao, L.-S. (2018). The role of fluorine-substitution on the π-bridge in constructing effective thermally activated delayed fluorescence molecules. J. Mater. Chem. C 6, 5536–5541.

Liang, Q., Xu, J., Xue, J., and Qiao, J. (2020). Near-infrared-II thermally activated delayed fluorescent organic light-emitting diodes. Chem. Commun. 56, 8988–8991.

Lin, T.A., Chatterjee, T., Tsai, W.L., Lee, W.K., Wu, M.J., Jiao, M., Pan, K.C., Yi, C.L., Chung, C.L., Wong, K.T., and Wu, C.C. (2016). Sky-blue organic light emitting diode with 37% external quantum efficiency using thermally activated delayed fluorescence from spiroacridine-triazine hybrid. Adv. Mater. 28, 6976–6983.

Madayanad Suresh, S., Hall, D., Beljonne, D., Olivier, Y., and Zysman-Colman, E. (2020). Multiresonant thermally activated delayed fluorescence emitters based on heteroatom-doped nanographenes: recent advances and prospects for organic light-emitting diodes. Adv. Funct. Mater. 30, 1908677.

Nagata, R., Nakanotani, H., and Adachi, C. (2017). Near-infrared electrophosphorescence up to 1.1 μm using a thermally activated delayed fluorescence molecule as triplet sensitizer. Adv. Mater. 29, 1604265.

Nakanotani, H., Higuchi, T., Furukawa, T., Masui, K., Morimoto, K., Numata, M., Tanaka, H., Sagara, Y., Yasuda, T., and Adachi, C. (2014). High-efficiency organic light-emitting diodes with fluorescent emitters. Nat. Commun. 5, 4016.

Ni, F., Li, N., Zhan, L., and Yang, C. (2020). Organic thermally activated delayed fluorescence materials for time-resolved luminescence imaging and sensing. Adv. Opt. Mater. 8, 1902187.

Pan, Y., Li, W., Zhang, S., Yao, L., Gu, C., Xu, H., Yang, B., and Ma, Y. (2014). High yields of singlet excitons in organic electroluminescence through two paths of cold and hot excitons. Adv. Opt. Mater. 2, 510–515.

Peng, C.-C., Yang, S.-Y., Li, H.-C., Xie, G.-H., Cui, L.-S., Zou, S.-N., Poriel, C., Jiang, Z.-Q., and Liao, L.-S. (2020). Highly efficient thermally activated delayed fluorescence via an unconjugated donor-acceptor system realizing EQE of over 30%. Adv. Mater. 32, 2003885.

Qi, J., Sun, C., Li, D., Zhang, H., Yu, W., Zebibula, A., Lam, J.W.Y., Xi, W., Zhu, L., Cai, F., et al. (2018). Aggregation-induced emission luminogen with near-infrared-II excitation and near-infrared-I emission for ultradeep intravital two-photon microscopy. ACS Nano 12, 7936–7945.

Qian, G., and Wang, Z.Y. (2010). Near-infrared organic compounds and emerging applications. Chem. Asian J. 5, 1006–1029.

Qian, G., Zhong, Z., Luo, M., Yu, D., Zhang, Z., Wang, Z.Y., and Ma, D. (2009). Simple and efficient near-infrared organic chromophores for light-emitting diodes with single electroluminescent emission above 1000 nm. Adv. Mater. 21, 111–116.

Samanta, P.K., Kim, D., Coropceanu, V., and Bredas, J.L. (2017). Up-conversion intersystem crossing rates in organic emitters for thermally activated delayed fluorescence: impact of the nature of singlet vs triplet excited states. J. Am. Chem. Soc. 139, 4042–4051.

Sarma, M., and Wong, K.T. (2018). Exciplex: an intermolecular charge-transfer approach for TADF. ACS Appl. Mater. Inter. 10, 19279–19304.

Shahalizad, A., Malinge, A., Hu, L., Laflamme, G., Haeberlé, L., Myers, D.M., Mao, J., Skene, W.G., and Kéna-Cohen, S. (2020). Efficient solution-processed hyperfluorescent OLEDs with spectrally narrow emission at 840 nm. Adv. Funct. Mater. 31, 2007119.

Shimizu, S. (2019). aza-BODIPY synthesis towards vis/NIR functional chromophores based on a Schiff base forming reaction protocol using lactams and heteroaromatic amines. Chem. Commun. 55, 8722–8743.

Sun, K., Chu, D., Cui, Y., Tian, W., Sun, Y., and Jiang, W. (2017). Near-infrared thermally activated delayed fluorescent dendrimers for the efficient non-doped solution-processed organic light-emitting diodes. Org. Electron. 48, 389–396.

Tang, C.W., and VanSlyke, S.A. (1987). Organic electroluminescent diodes. Appl. Phys. Lett. 51, 913–915.

Tang, X., Cui, L.-S., Li, H.-C., Gillett, A.J., Auras, F., Qu, Y.-K., Zhong, C., Jones, S.T.E., Jiang, Z.-Q.,

Friend, R.H., and Liao, L.-S. (2020). Highly efficient luminescence from space-confined charge-transfer emitters. Nat. Mater. 19, 1332–1338.

Tao, Y., Yuan, K., Chen, T., Xu, P., Li, H., Chen, R., Zheng, C., Zhang, L., and Huang, W. (2014). Thermally activated delayed fluorescence materials towards the breakthrough of organoelectronics. Adv. Mater. 26, 7931–7958.

Tsujimoto, H., Ha, D.G., Markopoulos, G., Chae, H.S., Baldo, M.A., and Swager, T.M. (2017). Thermally activated delayed fluorescence and aggregation induced emission with through-space charge transfer. J. Am. Chem. Soc. 139, 4894–4900.

Tuong Ly, K., Chen-Cheng, R.-W., Lin, H.-W., Shiau, Y.-J., Liu, S.-H., Chou, P.-T., Tsao, C.-S., Huang, Y.-C., and Chi, Y. (2016). Near-infrared organic light-emitting diodes with very high external quantum efficiency and radiance. Nat. Photon. 11, 63–68.

Uoyama, H., Goushi, K., Shizu, K., Nomura, H., and Adachi, C. (2012). Highly efficient organic light-emitting diodes from delayed fluorescence. Nature 492, 234–238.

Wada, Y., Nakagawa, H., Matsumoto, S., Wakisaka, Y., and Kaji, H. (2020). Organic light emitters exhibiting very fast reverse intersystem crossing. Nat. Photon. 14, 643–649.

Wang, S., Cheng, Z., Song, X., Yan, X., Ye, K., Liu, Y., Yang, G., and Wang, Y. (2017). Highly efficient long-wavelength thermally activated delayed fluorescence OLEDs based on dicyanopyrazino phenanthrene derivatives. ACS Appl. Mater. Inter. 9, 9892–9901.

Wang, S., Miao, Y., Yan, X., Ye, K., and Wang, Y. (2018). A dibenzo[a,c]phenazine-11,12-dicarbonitrile (DBPzDCN) acceptor based thermally activated delayed fluorescent compound for efficient near-infrared electroluminescent devices. J. Mater. Chem. C 6, 6698–6704.

Wang, S., Yan, X., Cheng, Z., Zhang, H., Liu, Y., and Wang, Y. (2015). Highly efficient near-infrared delayed fluorescence organic light emitting diodes using a phenanthrene-based charge-transfer compound. Angew. Chem. Int. Ed. 54, 13068–13072.

Wang, S., Zhang, H., Zhang, B., Xie, Z., and Wong, W.-Y. (2020). Towards high-power-efficiency solution-processed OLEDs: material and device perspectives. Mater. Sci. Eng. R. 140, 100547.

Wei, Y.-C., Wang, S.F., Hu, Y., Liao, L.-S., Chen, D.-G., Chang, K.-H., Wang, C.-W., Liu, S.-H., Chan, W.-H., Liao, J.-L., et al. (2020). Overcoming the energy gap law in near-infrared OLEDs by exciton-vibration decoupling. Nat. Photon. 14, 570–577.

Xu, Y., Li, C., Li, Z., Wang, Q., Cai, X., Wei, J., and Wang, Y. (2020). Constructing charge transfer excited state based on frontier molecular orbital engineering: narrowband green electroluminescence with high color purity and efficiency. Angew. Chem. Int. Ed. 59, 17442.

Xu, Y., Liang, X., Zhou, X., Yuan, P., Zhou, J., Wang, C., Li, B., Hu, D., Qiao, X., Jiang, X., et al. (2019). Highly efficient blue fluorescent OLEDs

based on upper level triplet-singlet intersystem crossing. Adv. Mater. *31*, 1807388.

Xue, J., Liang, Q.X., Zhang, Y.G., Zhang, R.Y., Duan, L., and Qiao, J. (2017). High-efficiency near-infrared fluorescent organic light-emitting diodes with small efficiency roll-off: a combined design from emitters to devices. Adv. Funct. Mater. *27*, 1703283.

Xue, J., Liang, Q., Wang, R., Hou, J., Li, W., Peng, Q., Shuai, Z., and Qiao, J. (2019). Highly efficient thermally activated delayed fluorescence via J-aggregates with strong intermolecular charge transfer. Adv. Mater. *31*, 1808242.

Yamanaka, T., Nakanotani, H., Hara, S., Hirohata, T., and Adachi, C. (2017). Near-infrared organic light-emitting diodes for biosensing with high operating stability. Appl. Phys. Express *10*, 074101.

Yang, M., Park, I.S., and Yasuda, T. (2020a). Full-Color, narrowband, and high-efficiency electroluminescence from boron and carbazole embedded polycyclic heteroaromatics. J. Am. Chem. Soc. *142*, 19468–19472.

Yang, S.-Y., Tian, Q.-S., Yu, Y.-J., Zou, S.-N., Li, H.-C., Khan, A., Wu, Q.-H., Jiang, Z.-Q., and Liao, L.-S. (2020b). Sky-blue thermally activated delayed fluorescence with intramolecular spatial charge transfer based on a dibenzothiophene sulfone emitter. J. Org. Chem. *85*, 10628–10637.

Yang, S.-Y., Wang, Y.-K., Peng, C.-C., Wu, Z.-G., Yuan, S., Yu, Y.-J., Li, H., Wang, T.-T., Li, H.-C., Zheng, Y.-X., et al. (2020c). Circularly polarized thermally activated delayed fluorescence emitters in through-space charge transfer on asymmetric spiro skeletons. J. Am. Chem. Soc. *142*, 17756–17765.

Yang, Z., Mao, Z., Xie, Z., Zhang, Y., Liu, S., Zhao, J., Xu, J., Chi, Z., and Aldred, M.P. (2017). Recent advances in organic thermally activated delayed fluorescence materials. Chem. Soc. Rev. *46*, 915–1016.

Ye, H., Kim, D.H., Chen, X.K., Sandanayaka, A.S.D., Kim, J.U., Zaborova, E., Canard, G., Tsuchiya, Y., Choi, E.-Y., Wu, J.W., et al. (2018). Near-infrared electroluminescence and low threshold amplified spontaneous emission above 800 nm from a thermally activated delayed fluorescent emitter. Chem. Mater. *30*, 6702–6710.

Yu, Y.J., Hu, Y., Yang, S.Y., Luo, W., Yuan, Y., Peng, C.C., Liu, J.F., Khan, A., Jiang, Z.Q., and Liao, L.S. (2020). Near-infrared electroluminescence beyond 800 nm with high efficiency and radiance from anthracene cored emitters. Angew. Chem. Int. Ed. *59*, 21578.

Yuan, Y., Hu, Y., Zhang, Y.X., Lin, J.D., Wang, Y.K., Jiang, Z.Q., Liao, L.S., and Lee, S.T. (2017). Over 10% EQE near-infrared electroluminescence based on a thermally activated delayed fluorescence emitter. Adv. Funct. Mater. *27*, 1700986.

Zampetti, A., Minotto, A., and Cacialli, F. (2019). Near-Infrared (NIR). organic light-emitting diodes (OLEDs): challenges and opportunities. Adv. Func. Mater. *29*, 1807623.

Zeng, W., Lai, H.Y., Lee, W.K., Jiao, M., Shiu, Y.J., Zhong, C., Gong, S., Zhou, T., Xie, G., Sarma, M., et al. (2018). Achieving nearly 30% external quantum efficiency for orange-red organic light emitting diodes by employing thermally activated delayed fluorescence emitters composed of 1,8-naphthalimide-acridine hybrids. Adv. Mater. *30*, 1704961.

Zhang, Q., Kuwabara, H., Potscavage, W.J., Jr., Huang, S., Hatae, Y., Shibata, T., and Adachi, C. (2014). Anthraquinone-based intramolecular charge-transfer compounds: computational molecular design, thermally activated delayed fluorescence, and highly efficient red electroluminescence. J. Am. Chem. Soc. *136*, 18070–18081.

Zhang, Y.L., Ran, Q., Wang, Q., Liu, Y., Hanisch, C., Reineke, S., Fan, J., and Liao, L.S. (2019). High-efficiency red organic light-emitting diodes with external quantum efficiency close to 30% based on a novel thermally activated delayed fluorescence emitter. Adv. Mater. *31*, 1902368.

Zhang, Y.M., Wang, Y.F., Song, J., Qu, J.L., Li, B.H., Zhu, W.G., and Wong, W.Y. (2018). Near-Infrared emitting materials via harvesting triplet excitons: molecular design, properties, and application in organic light emitting diodes. Adv. Opt. Mater. *6*, 1800466.

Zhang, Y., Song, J., Qu, J., Qian, C.-P., and Wong, W.-Y. (2020a). Recent progress of electronic materials based on 2,1,3-benzothiadiazole and its derivatives: synthesis and their application in organic light-emitting diodes. Sci. China Chem. https://doi.org/10.1007/s11426-020-9901-4.

Zhang, Y., Zhang, D., Huang, T., Li, G., Zhang, C., Lu, Y., Liu, Z., and Duan, L. (2020b). Beating the limitation of energy gap law utilizing deep red MR-TADF emitter with narrow energy-bandwidth. Chemrxiv. Preprint. https://doi.org/10.26434/chemrxiv.13202975.v1.

Zhang, M., Zheng, C.-J., Lin, H., and Tao, S.-L. (2021). Thermally activated delayed fluorescence exciplex emitters for high-performance organic light-emitting diodes. Mater. Horiz. https://doi.org/10.1039/D0MH01245A.

Zhao, B., Xie, G., Wang, H., Han, C., and Xu, H. (2019). Simply structured near-infrared emitters with a multicyano linear acceptor for solution-processed organic light-emitting diodes. Chem. Eur. J. *25*, 1010–1017.

Zhao, Z., Zhang, H., Lam, J.W.Y., and Tang, B.Z. (2020). Aggregation-induced emission: new vistas at the aggregate level. Angew. Chem. Int. Ed. *59*, 9888–9907.